arXiv:1411.5522v1 [astro-ph.CO] 20 Nov 2014

The Cosmological Effect of CMB/BAO Measurements

Yi Zhang [a,b,1]

[a] *College of Science, Chongqing University of Posts and Telecommunications, Chongqing 400065, China*

[b] *State Key Laboratory of Theoretical Physics, Institute of Theoretical Physics, Chinese Academy of Science, Beijing 100190, China*

Abstract

In this paper, the CMB/BAO measurements which cover the 13 redshift data in the regime $0.106 \leq z \leq 2.34$ are given out. The CMB/BAO samples are based on the BAO distance ratios $r_s(z_d)/D_V(z)$ and the CMB acoustic scales l_A. It could give out the accelerating behaviors of the ΛCDM, wCDM and oΛCDM models. As the direction of the degeneracy of $\Omega_{m0} - w$ and $\Omega_{m0} - \Omega_{k0}$ are different for the CMB/BAO and BAO data, the CMB/BAO data show ability of breaking parameter degeneracy. Our tightest constraining results is from the BAO+Planck/BAO+$\Omega_b h^2$+$\Omega_m h^2$ data which has Ω_{m0} tension, but doesn't have H_0 tension with the Planck result. The extending parameters w and Ω_{k0} could alleviate the Ω_{m0} tensions slightly.

[1]Email: zhangyia@cqupt.edu.cn

1 Introduction

The CMB/BAO data [1] is a kind of observational data which try to exact more information from the important cosmological experiments: CMB (Cosmic Microwave Background) and BAO (Baryon Acoustic Oscillation). The CMB probes the rate of the expansion at redshift $z \sim 1100$ [2, 3] and the BAO technique provides a distance-redshift relation at low redshifts [4, 5, 6, 7, 8, 9, 10, 11, 12, 13, 14, 15, 16]. CMB and BAO are observations to different issues and challenges, and affected by different physics; one is by any non-standard early-universe physics, the other is by late time expansion mainly. Typically, the CMB/BAO cosmological constraining results are discussed with other low-redshift data or the CMB data to fix tightly constraining portions of parameter space. In this letter, the CMB/BAO data is sufficient to permit a meaningful comparison with type IA supernovae (SNe) measurement without strong CMB priors.

In the first CMB/BAO paper [1], the number of CMB/BAO data is just 2. As the development of BAO survey, and the number is increased to 5 in Refs.[2, 17, 18]. To make clear the constraining effects of the CMB/BAO data, here we collect 13 observational BAO data and choose the Planck or WMAP9 survey[2]. One benefit of the BAO data is that it is limited by the statistical error, rather than systematic uncertainties [20]. As the newly released CMB data, Planck results, consist with the results from BAOs data [22]. We concentrate on testing the ΛCDM model and its extensions with the CMB/BAO data.

The rationale for considering the ΛCDM model is that one could consider the cosmological constant as a "null hypothesis" for dark energy, so it is worth exploring whether it provides a reasonable description of data. As our dataset larger, whether the dataset is suitable to standard ΛCDM model is an interesting question. And, a hypothetical deviation from Λ-acceleration may first appear as a tension between CMB and low-redshift data, or arise from statistical fluctuations, systematic uncertainties that are incorrectly correctly quantified, alternatively extensions to the standard model, or some combinations of these factors. The ability to disambiguate these possibilities from current and future low-redshift experiments is crucial. So we consider wCDM which adopted a constant w (the equation of state of dark energy p_{de}/ρ_{de}) and oΛCDM model which extends this model to non-zero dimensionless energy density of curvature Ω_{k0} as well.

In this paper, we use improved CMB/BAO data to constrain the ΛCDM, wCDM and

[2]In the simulated BAO data which has 21 data [19], the ΛCDM model could be constrained as well.

ΛCDM models. The rest of the paper is organized as follows. In Section 2, we update the CMB/BAO data and give out the theoretical models. In Section 3, we compare the constraining result and discuss the effects of the CMB and BAO data. At last, we present a short summary in Section 4.

2 Data

The acoustic peak in the galaxy correlation function provides a standard ruler $r_s(z_d)/D_V(z)$ (or its inverse $D_V(z)/r_s(z_d)$) which measure the distance to objects at redshift z of recombination in unit of the sound horizon. The sound horizon and the dubbed spherically averaged distance are

$$r_s(z_d) = \int_{z_d}^{\infty} \frac{c_s(z)dz}{H(z)},$$
$$D_V(z) = (\frac{(1+z)^2 d_A(z_*)^2 cz}{H})^{1/3},$$

where H is the Hubble parameter, c_s is the speed of sound before recombination, $d_A(z_*)$ is the co-moving angular diameter distance to recombination, z_* is the redshift at recombination with the value of 1090.48 and z_d is the value of the redshift of the drag epoch which is gotten by the fitting formula in Ref.[21]. The observable quantities of BAO are only sensitive to the early universe physics via the sound horizon $r_s(z_d)$. And, the CMB data provide an excellent standard ruler as well which is the position of the first CMB power spectrum peak which represents the angular scale of sound horizon at recombination z_*, dubbed the acoustic scale,

$$l_A = \frac{\pi d_A(z_*)(1+z_*)}{r_s(z_*)}.$$

The CMB/BAO parameter f is regarded to be more suitable than the primitive CMB shift parameter l_A for non-standard dark energy model [1, 17, 18]:

$$f(z) = \frac{l_A}{\pi} * \frac{r_s}{D_V(z)} * \frac{r_s(z_*)}{r_s(z_d)} = \frac{d_A(z_*)}{D_V(z)},$$
$$\frac{\sigma_f}{f} = \sqrt{(\frac{\sigma_{l_A}}{l_A})^2 + (\frac{\sigma_{BAO}}{r_s(z_*)/D_V(z)})^2 + (\frac{\sigma_{r_s(z_d)/r_s(z_*)}}{r_s(z_d)/r_s(z_*)})^2},$$

where σ presents the error bar. And f is regarded to have the ability of removing the dependence on much of the complex pre-recombination physics which is needed to determine the horizon scale. In the following, we introduce the BAO and CMB samples separately.

Redshift z	$r_s(z_d)/D_V(z)$	f(Planck/BAO)	f(WMAP9/BAO)	f(WMAP9(w)/BAO)	BAO)
0.106	0.336 ± 0.015	31.56 ± 1.44	30.82 ± 1.43	30.85 ± 1.43	Ref. [5] 6dFGS
0.20	0.1905 ± 0.0061	17.95 ± 0.60	17.53 ± 0.60	17.54 ± 0.60	Ref.[6] SDSS LRG
0.35	0.1097 ± 0.0036	10.33 ± 0.35	10.09 ± 0.35	10.10 ± 0.35	Ref.[6] SDSS LRG
0.275	0.1390 ± 0.0037	13.09 ± 0.37	12.79 ± 0.37	12.80 ± 0.37	Ref.[6]SDSS LRG
0.278	0.1389 ± 0.0043	13.08 ± 0.42	12.78 ± 0.42	12.79 ± 0.42	Ref.[7] SDSS LRG
0.35	0.1126 ± 0.0022	10.61 ± 0.23	10.36 ± 0.24	10.37 ± 0.24	Ref.[8] SDSS LRG
0.314	0.1239 ± 0.0033	11.67 ± 0.33	11.40 ± 0.33	11.41 ± 0.33	Ref.[9] SDSS LRG
0.44	0.0916 ± 0.0071	8.63 ± 0.67	8.43 ± 0.66	8.44 ± 0.66	Ref.[9] Wigglez
0.60	0.0726 ± 0.0034	6.84 ± 0.33	6.68 ± 0.32	6.69 ± 0.32	Ref.[9] Wigglez
0.73	0.0592 ± 0.0032	5.58 ± 0.31	5.45 ± 0.30	5.45 ± 0.30	Ref.[9] Wigglez
0.32	0.1212 ± 0.0024	11.42 ± 0.25	11.15 ± 0.26	11.16 ± 0.26	Ref.[10] BOSS DR11
0.57	0.0732 ± 0.0012	6.90 ± 0.13	6.73 ± 0.14	6.74 ± 0.14	Ref.[10] BOSS DR11
2.34	0.0320 ± 0.0007	3.01 ± 0.07	2.94 ± 0.07	2.95 ± 0.07	Ref.[11]BOSS DR11

Table 1: The BAO and CMB/BAO samples are derived from 6dFGS, SDSS LRG, WiggleZ, BOSS DR11, Planck and WAMP9. Explanation please see Section 2.

2.1 The BAO distance ratio

We list the BAO data $r_s(z_d)/D_V(z)$ in Table 1 which are derived from the 6dF Galaxy Redshift Survey (6dFGS), Sloan Digital Sky Survey Luminous Red Galaxy sample ((SDSS LRG) , WiggleZ, Baryon Oscillation Spectroscopic Survey (BOSS) DR11 surveys[3]. The $r_s(z_d)/D_V(z)$ data have now been detected over a range of redshifts from $z = 0.106$ to $z = 2.34$.

(1) Beutler et al. analyzed the large-scale correlation function of the 6dFGS and made a 4.5 percent measurement at z = 0.106 [5].

(2) Percival et al. measured the distance ratio $d_z = r_s(z_d)/D_V(z)$ at redshifts $z = 0.2$, and $z = 0.35$ by fitting to the power spectra of luminous red galaxies and main-sample galaxies in the SDSS [6]. They also showed how the distance-reshift constraints at those two redshifts could be decomposed into a single distance constant at $z = 0.275$ and a "gradient" around this pivot given by $D_V(0.35)/D_V(0.2)$. Furthermore, Kazin et al. examined the correlation function ξ of the SDSS LRG at large scales using the final data release and get the BAO data at $z = 0.278$ [7]. Furthermore, Padmanabhan et al. applied the reconstruction technique to the clustering of galaxies from the SDSS LRG sample, sharpening the BAO feature and achieving the BAO result for z = 0.35 [8].

(3) Blake et al. gave out the BAO feature in three bins centered at redshifts z = 0.44, 0.60, and 0.73 respectively, using the full sample of 158741 galaxies from WiggleZ survey. And they also presented a new measurement of the baryon acoustic feature in the correlation

[3] Our BAO data only use the distance ratio, not the other BAO parameter, e.g. the acoustic parameter A. Thus, our BAO-only constraining results is different from the result of Ref.[22, 23, 24].

function of the SDSS LRG sample and derived a BAO measurement at $z = 0.314$ that is consistent with previous analyses of the LRG power spectrum [9].

(4) Fitting for the position of the acoustic features in the correlation function and matter power spectrum of BAO in the clustering of galaxies from BOSS DR 11, Anderson et al. got the BAO result for $z = 0.32$ and $z = 0.57$ [10]. And from BOSS DR11 latest released sample, Delubac et al. figured out the BAO feature in the flux-correction function of the Lyman-α forest of high reshift quasars at the effective redshift $z = 2.34$ [11].

2.2 The acoustic scale

While the CMB anisotropies have been measured with ever increasing precision by missions such as WMAP9 [2], Planck [3] and BICEP2 [25]. Sepcially, the declaration that the detect on of the CMB B-mode polarization by the BICEP2 collaboration [25] might be wholly or partly due to polarized dust emission [26]. For conciseness, we choose the Planck and WMAP9 data only. Indeed, the l_A parameter depends on the background model sightly [30]. The used acoustic scale $l_A(z_*)$ and $r_s(z_d)/r_s(z_*)$ at the decoupling redshift derived by Refs [27, 28] :

$$Planck + lensing + WP : l_A = 301.57 \pm 0.18(0.06\%), \frac{r_s(z_d)}{r_s(z_*)} = 1.019 \pm 0.009(0.88\%),$$
$$WMAP9 : \quad l_A = 302.02 \pm 0.66(0.22\%), \quad \frac{r_s(z_d)}{r_s(z_*)} = 1.045 \pm 0.012(1.15\%),$$
$$WMAP9(w) : \quad l_A = 302.35 \pm 0.65(0.21\%), \quad \frac{r_s(z_d)}{r_s(z_*)} = 1.045 \pm 0.012(1.15\%).$$

The First CMB data combined with Planck lensing, as well as WMAP polarization at low multipoles ($l \leq 23$) [3] which represents the tightest constraints from CMB data only at present. The second one is derived from the oΛCDM model [27, 28] and WMAP9 data. The third one derived from the owCDM model [2] and WMAP9 data. To distinguish the three kinds of CMB/BAO data, we call them Planck/BAO, WMAP9/BAO, and WMAP9(w)/BAO separately. As Ref.[30] shows, the l_A values vary if changing the fitting model. Our results will show the value of l_A nearly don't affect the constraining results.

Based on BAO and CMB data, our CMB/BAO sample has 13 data which are presented in Table 1. The WMAP9(w)/BAO data cove the total 5 CMB/BAO in Ref.[17]. Comparing the error in the BAO data, obviously, the CMB data will bring less uncertainty than BAO to the CMB/BAO, but the whole CMB/BAO data uncertainty has larger error than the

BAO data. Our results will show a tighter constraint from the CMB/BAO data compared with BAO data in Table 2.

2.3 The theoretical models

This accelerating behavior of our universe is usually attributed by a presently unknown component, called dark energy, which exhibits negative pressure and dominates over the matter-energy content of our universe. So far, the simplest candidate for dark energy is the cosmological constant. And, the so called standard cosmological model ΛCDM is in accordance with almost all the existing cosmological observations. As the CMB/BAO method retains sensitivity to phenomena that have more effect at higher redshift, such as curvature, we extend the constraining model to wCDM (the standard cosmological model with constant dark energy equation of state) and oΛCDM (the standard cosmological model with curvature). It means we use the following parameters: the equation of state of dark energy w, Hubble parameter H, and the dimensionless energy density parameter for the matter Ω_{m0} and the curvature Ω_{k0}.

The BAO position measurements do not provide any H_0 constraint, being sensitive only to the combination $H_0 r_s$. The sound horizon depends on the physical baryon density, $\Omega_b h^2$, through $r_s \propto (\Omega_b h^2)^{-0.13}$. We then add the prior $\Omega_b h^2 = 0.0223 \pm 0.0009$ [34] to the BAO data by fixing the CMB mean temperature, which is fixed to $2.73K$ and determines the energy density in radiation. On the other side, the CMB/BAO data is independent from the sound horizon, thus CMB/BAO-only data could not constrain H_0. Correspondingly, we add the $\Omega_m h^2 = 0.1199 \pm 0.0027$ prior from Planck to the CMB/BAO for the H_0 constraint.

For data comparison convenience, we divide the data into three samples:(1) the CMB related data Planck/BAO (or $+\Omega_m h^2$), WMAP/BAO (or $+\Omega_m h^2$), WMAP(w)/BAO (or $+\Omega_m h^2$); (2) the BAO data related data: BAO (or $+\Omega_b h^2$), BAO+Planck/BAO (or $+\Omega_b h^2$), BAO+WMAP/BAO (or $+\Omega_b h^2$); (3) all combined data: BAO+Planck/BAO $+\Omega_b h^2 + \Omega_m h^2$, BAO+WMAP/BAO $+\Omega_b h^2 + \Omega_m h^2$. And, we use the Monte Carlo Markov Chain (MCMC) method based on the publicly available package COSMOMC [29] to constrain model parameters which randomly chooses values for the above parameters, evaluates χ^2 and determines whether to accept or reject the set of parameters by using the Metropolis-Hastings algorithm.

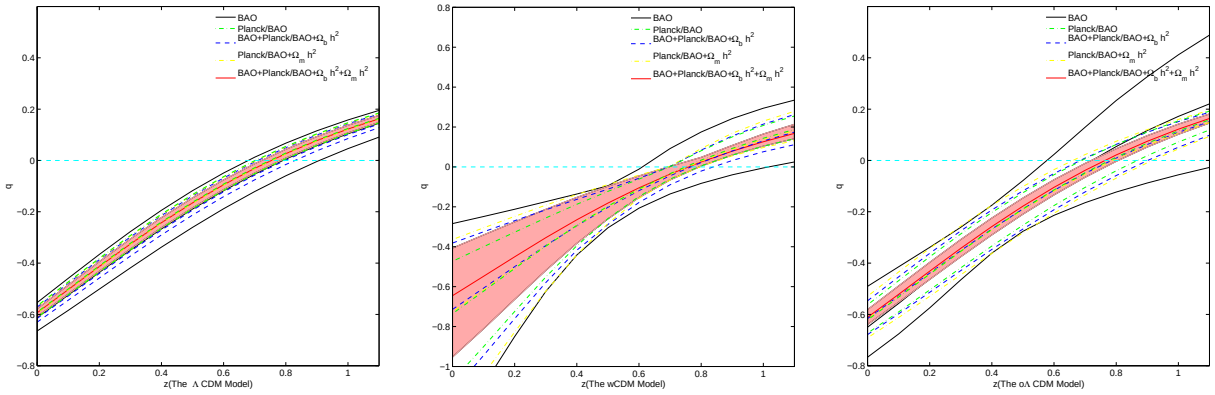

Figure 1: The evolution of the deceleration parameter q vs the redshift z for selected data.

3 Data Discussions and Parameter Comparisons

We report mean parameter values and boundaries of the symmetric 68% and 95% (1σ and 2σ confidence intervals (C.L.)) for all the models in Table 2. Before further analysis, we explain the value of χ^2 firstly. The BAO-only data obtain $\chi^2 = 2.272$ in the ΛCDM model, and the Planck/BAO data give $\chi^2 = 1.986$. Considering the numbers of the BAO and CMB/BAO data are both 13, the χ^2 is too small. And, limited improvement of χ^2 is given out after adding the $\Omega_b h^2$ prior and extending the ΛCDM model. Ref.[22] concluded this phenomenon is because parricidal overlap in both redshift and sky coverage for WiggleZ and BOSS. As we neglect interdependence between constraints from different surveys, our overlap dataset also have the same small χ^2.

Basically, all the data are effective to give out an accelerating universe which are shown in Figure 1. The derived decelerating parameter $q(z) = -a\ddot{a}/\dot{a}^2$ represents an accelerating universe when $-1 < q_0 < 0$. And the transition redshift z_t where $q(z_t) = 0$ denotes the time when our universe evolved from cosmic deceleration ($q > 0$) to acceleration($q < 0$). As a representative, the Planck/BAO data obtain

$$q_0 = -0.62^{+0.04+0.06}_{-0.01-0.02}, z_t = 0.80^{+0.03+0.05}_{-0.09-0.11}(\Lambda CDM),$$
$$q_0 = -0.71^{+0.33+0.47}_{-0.41-0.68}, z_t = 0.77^{+0.07+0.09}_{-0.07-0.13}(wCDM),$$
$$q_0 = -0.62^{+0.07+0.12}_{-0.06-0.10}, z_t = 0.80^{+0.13+0.22}_{-0.13-0.21}(o\Lambda CDM).$$

q_0 and z_t constraints have nearly identical central value to the most constraining result of $BAO + Planck/BAO + \Omega_m h^2 + /\Omega_b h^2$, but with larger error. Specially, the wCDM model gives out the latest transfer redshift and its deceleration parameter is smaller than the ones

in the ΛCDM and oΛCDM models. It is because the fitting value of w is less than -1, the universe is accelerating faster.

In general, the ΛCDM give out the tightest constraint while the extended parameter w and Ω_{k0} enlarge the parameter space. Although the chosen procedure is different, it is clear that the BAO+CMB/BAO+$\Omega_b h^2$+$\Omega_m h^2$ data make the main effect of tightening the parameter region. And to investigate the CMB and BAO effect separately, we plot the best fit value and parameter contours in Figure 2. The constraining results for all the models are nearly the same between WMAP9/BAO and WMAP9(w)/BAO data for Ω_{m0}, and just have a small difference for Ω_{k0} and w. The WMAP9(w)/BAO data could be replaced by the WMAP9/BAO data. Meanwhile, there are obvious shifts between the Planck/BAO and WMAP9/BAO data for the Ω_{m0}, Ω_{k0} and w parameters. The Planck and WMAP9 survey bring different l_A and $r_s(z_d)/r_s(z_*)$ while the WMAP9/BAO and WMAP9(w)/BAO have the same $r_s(z_d)/r_s(z_*)$. The result of Planck/BAO, WMAP9/BAO and WMAP9(w)/BAO are expected because the error for $r_s(z_d)/r_s(z_*)$ is 1% while that for l_A is 0.02%. And, the different results between Planck/BAO and WMAP9/BAO show through the recombination history not related to the CMB/BAO data directly, it determined the value and error of the CMB/BAO data.

3.1 The Ω_{m0} parameter

For the ΛCDM model, the BAO+Planck/BAO+$\Omega_b h^2$+$\Omega_m h^2$ data give out $\Omega_{m0} = 0.271^{+0.011+0.016}_{-0.010-0.015}$ which has a obvious tension with the Planck+WP+highL+BAO result where $\Omega_{m0} = 0.308 \pm 0.010(68\%)$. And, our result has a tension with the SNLS data which shows $\Omega_{m0} = 0.227^{+0.042}_{-0.035}(68\%)$, so is the Planck result. The tension between Planck and SNLS could be regarded as the systematics in SNLS SNe IA data, so it could be also used to explain pour results. And our results is consistent with the Union2.1 data where $\Omega_{m0} = 0.295^{+0.043}_{-0.040}(68\%)$ and the JLA data where $\Omega_{m0} = 0.295 \pm 0.034(68\%)$[4]. The tension of Ω_{m0} between the Planck data and our results could be alleviated by extending parameters. The BAO+Planck/BAO+$\Omega_b h^2$+$\Omega_m h^2$ data give out $\Omega_{m0} = 0.267^{+0.022+0.031}_{-0.024-0.035}$ for the wCDM model. Anyway, the final solution to the tension problem should consider the recombination history because the best fit of Ω_{m0} of the BAO+WMAP9/BAO+$\Omega_b h^2$+$\Omega_m h^2$ data is shifted for the ΛCDM and wCDM models compared to the BAO+Planck/BAO+$\Omega_b h^2$+$\Omega_m h^2$ data.

[4] JLA is obtained from the joint analysis of the SDSS-II and SNLS (Supernova Legacy Survey three year sample) collaborations.

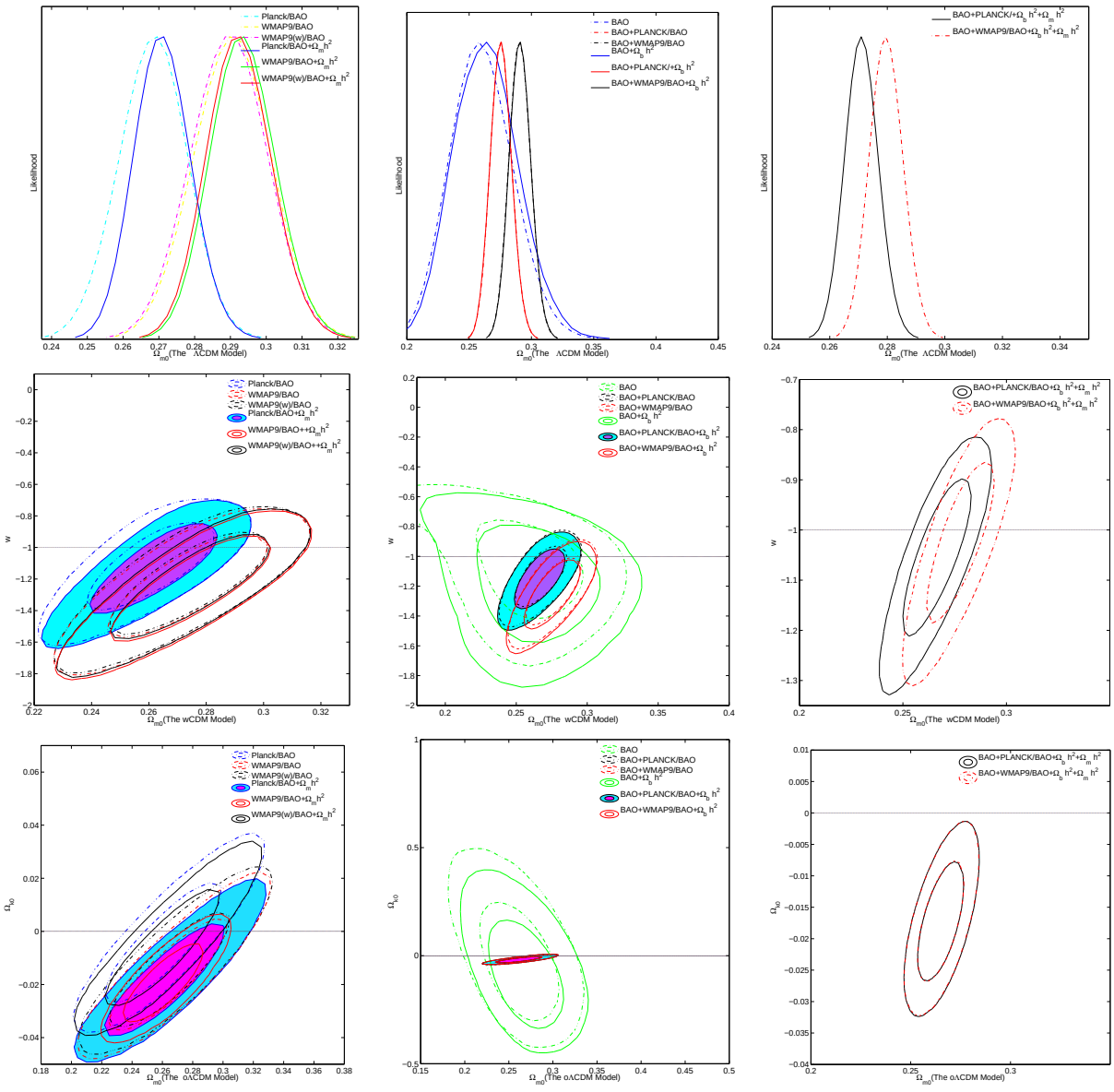

Figure 2: The upper three panels are the values of the likelihood of the parameter Ω_m for the ΛCDM model. The middle three panels in the transverse direction are the contour plots of $\Omega_{m0}-w$ for the wCDM model. The lower three panels are the contour plots of $\Omega_{m0}-\Omega_{k0}$ for the oΛCDM model. The left, middle and right three panels are for CMB comparison, BAO comparison and tightest constraint displaytion. The lines $w=-1$ and $\Omega_{k0}=0$ show the fixed values in the ΛCDM model.

3.2 The extended parameter w and Ω_{k0}

Both the CMB/BAO-only and BAO-only data give a very weak constrain on Ω_{k0} and w. Luckily, they yield different degeneracy directions for $\Omega_{m0} - w$ and $\Omega_{m0} - \Omega_{k0}$ which are slightly positive degenerated in CMB/BAO which means when Ω_{m0} inceases, w increases, but negative degenerated in BAO means when Ω_{m0} increases, w decreases. The BAO+CMB/BAO data give out a much tighter constraints and favor the CMB/BAO direction slightly for both Ω_{k0} and w as Figure 2 shows.

And due to the two-dimensional geometric degeneracy, the Planck+WP+BAO data alone constrain the range of the EOS of dark energy as $w = -1.13^{+0.24}_{-0.25}(95\%)$. Similarliy, our results of BAO+Planck/BAO+$\Omega_b h^2$+$\Omega_m h^2$ show $w = -1.042^{+0.196+0.267}_{-0.242-0.357}$. Comparing the contours and the $w = -1$ line in Figure 2, our results slightly favor phantom where $w < -1$.

The CMB curvature power spectrum measurements suffer from a well-known "geometrical degeneracy" which is broken via the integrated Sachs-Wolfe (ISW) effect on large angular scales and gravitational lensing of the CMB spectrum. And with the addition of probes of late time physics, the geometrical degeneracy can be broken as well. Our CMB/BAO results show it could constrain the curvature effectively which favor a small negative Ω_{k0} with the precision of 10^{-2}. The accuracy of the BAO+Planck/BAO+$\Omega_b h^2$+$\Omega_m h^2$ results which show $\Omega_{k0} = -0.017^{+0.020}_{-0.018}(95\%)$ is close to the Planck+Lensing+WP+highL result where $\Omega_{k0} = -0.01^{+0.018}_{-0.019}(95\%)$, but has larger error than the Planck+Lensing+WP+highL+BAO results where $\Omega_{k0} = -0.001^{+0.0062}_{-0.0065}(95\%)$.

3.3 The H_0 parameter

Adding the $\Omega_b h^2$ (or $\Omega_m h^2$) prior only affects the Ω_{m0} w and Ω_{k0} parameters slightly as Figures 2 shows, but it affects the H_0 parameter heavily as Figure 3 shows. To do effective containing, we set a range of H_0: $30\,km\,s^{-1}\,Mpc^{-1} \leq H_0 \leq 90 km s^{-1} Mpc^{-1}$. Table 2 shows the BAO data only give a lower bound to the H_0 which is around 40. After plus the $\Omega_b h^2$ prior, the accuracy of H_0 is increased to 5% as Figures 3 shows. And, the constraint tendency between $H_0 r_s$ and H_0 are the same which indicates the H_0 constraint is brought by the $\Omega_b h^2$ prior. On the other hand, the CMB/BAO data could not constrain the H_0 before adding the $\Omega_m h^2$ prior. The Planck/BAO+$\Omega_m h^2$ gives out the $66.6^{+1.8+2.9}_{-2.5-3.7}\,km\,s^{-1}\,Mpc^{-1}$ which is tighter than the BAO+ $\Omega_b h^2$ data. As for the degeneracy between $\Omega_{m0} - H_0$, Figure

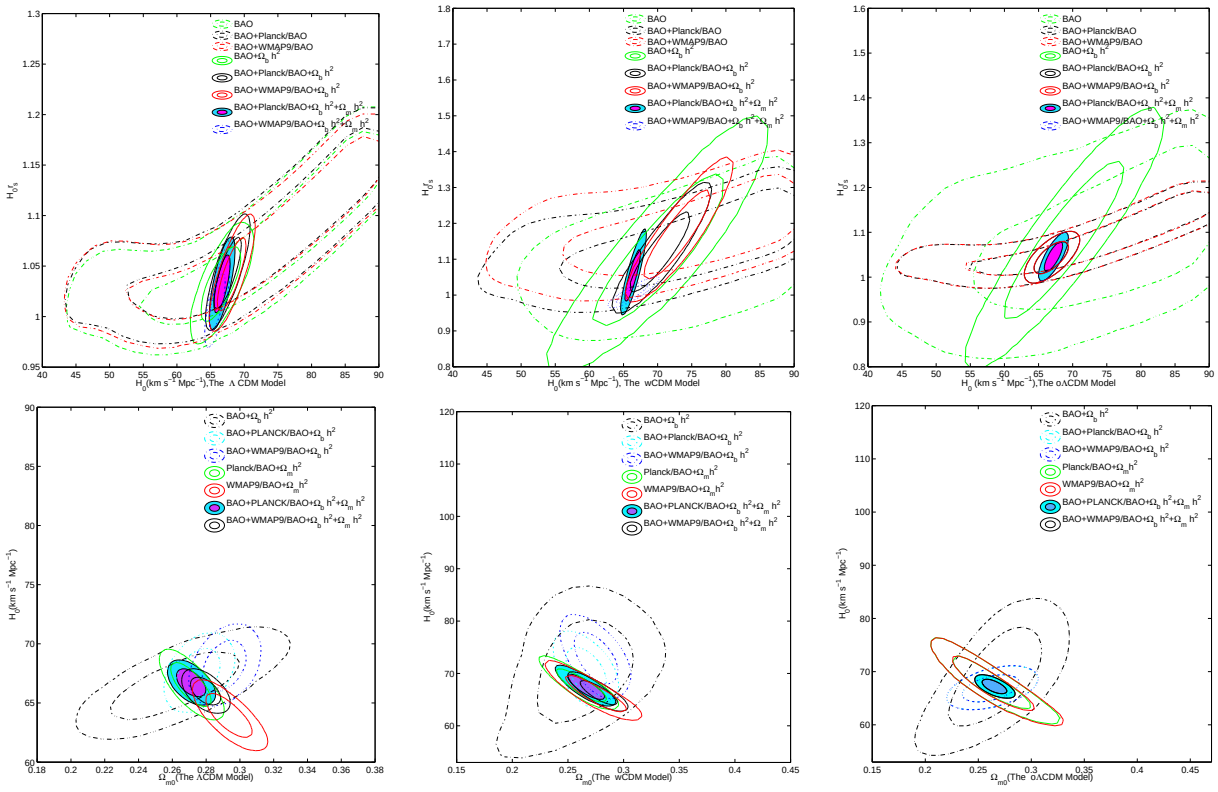

Figure 3: The upper and lower three panels are the contour plots of $H_0 r_s - H_0$ and $H_0 - \Omega_{m0}$ separatly for the Λ CDM, wCDM and oΛ CDM models.

3 shows BAO and CMB/BAO related data yield different degeneracy directions. They are slightly positive corrected in BAO related data, but negative related in CMB/BAO. And the CMB/BAO+BAO data favor the CMB/BAO direction.

The Planck+WP+highL results get $H_0 = (67.3 \pm 1.2)\, km\, s^{-1}\, Mpc^{-1}$ (68%). And, the local distance ladder measurements obtain $H_0 = (73.8 \pm 2.4) kms^{-1} Mpc^{-1}$ measured using Cepheid variable stars and low-redshift type IA SNe observed with the Hubble Space Telescope (HST) by Refs. [32, 33]. Our $BAO + Planck/BAO + \Omega_b h^2 + \Omega_m h^2$ results show $66.7^{+1.4+2.1}_{-1.4-2.1}\, km\, s^{-1}\, Mpc^{-1}$ which does not have tension with the Planck results, but has mild tensions with local distance ladder measurement of H_0 in the context of ΛCDM model. The tension come either from some sources of unknown systematic errors in some astrophysical measurements or the wrong ΛCDM model applied in fitting the data. After adding the parameter Ω_{k0} and w, this tension is alleviated slightly in our results where the parameter Ω_{k0} and w enlarge the H_0 range.

4 Short Summary

Here we obtain CMB/BAO samples with 13 data in the range of $0.106 \leq z \leq 2.34$ and focus on parameter constraints and model tests. Basically, the CMB/BAO data give out a tighter constraint compared to the BAO data though its error increased. As the degeneracies of $\Omega_{m0} - w$ and $\Omega_{m0} - \Omega_{k0}$ are positive for the CMB/BAO data while it is negative for the BAO distance ratio data.

Fitting the theoretic models to the BAO+Planck/BAO+$\Omega_b h^2$+$\Omega_m h^2$ data , we get constraints on ΛCDM model as $\Omega_{m0} = 0.271^{+0.011+0.016}_{-0.010-0.015}$ and $H_0 = 66.7^{+1.4+2.1}_{-1.4-2.1}\, km\, s^{-1}\, Mpc^{-1}$; constraints on the wΛCDM model as $\Omega_{m0} = 0.267^{+0.022+0.031}_{-0.024-0.035}$, $w = -1.042^{+0.196+0.267}_{-0.242-0.357}$ and $H_0 = 67.3^{+3.6+5.4}_{-3.0-4.2}\, km\, s^{-1}\, Mpc^{-1}$ and constraints on the oΛCDM model from the Planck/CMB as $\Omega_{m0} = 0.265^{+0.017+0.024}_{-0.016-0.022}$, $\Omega_{k0} = -0.017^{+0.014+0.020}_{-0.013-0.018}$ and $H_0 = 67.2^{+1.9+2.7}_{-1.9-2.6}\, km\, s^{-1}\, Mpc^{-1}$.

All our data about Ω_{m0} have tension with the Planck result, but consistent with the SNe data. As for H_0, our result is consistent with the Planck data, but has tension with the local measurements. And, our results slightly favor phantom dark energy where $w < -1$ and a negative Ω_{k0}.

5 Acknowledgements

The author thank Dr. Hui Li and Dr. Zhengxiang Li for useful discussions. This work was supported by the National Natural Science Foundation of China key project under grant No. 10935013, and CQ CSTC under grant No. 2010BB0408.

References

[1] J. Sollerman *et al.*, Astrophys. J. **703**, 1374 (2009) [arXiv:0908.4276 [astro-ph.CO]].

[2] C. L. Bennett *et al.* [WMAP Collaboration], Astrophys. J. Suppl. **208**, 20 (2013) [arXiv:1212.5225 [astro-ph.CO]].

[3] P. A. R. Ade *et al.* [Planck Collaboration], arXiv:1303.5076 [astro-ph.CO].

[4] W. J. Percival, S. Cole, D. J. Eisenstein, R. C. Nichol, J. A. Peacock, A. C. Pope and A. S. Szalay, Mon. Not. Roy. Astron. Soc. **381**, 1053 (2007) [arXiv:0705.3323 [astro-ph]].

[5] F. Beutler *et al.*, Mon. Not. Roy. Astron. Soc. **416**, 3017 (2011) [arXiv:1106.3366 [astro-ph.CO]].

[6] W. J. Percival *et al.* [SDSS Collaboration], Mon. Not. Roy. Astron. Soc. **401**, 2148 (2010) [arXiv:0907.1660 [astro-ph.CO]].

[7] E. A. Kazin *et al.* [SDSS Collaboration], Astrophys. J. **710**, 1444 (2010) [arXiv:0908.2598 [astro-ph.CO]].

[8] N. Padmanabhan, X. Xu, D. J. Eisenstein, R. Scalzo, A. J. Cuesta, K. T. Mehta and E. Kazin, Mon. Not. Roy. Astron. Soc. **427**, no. 3, 2132 (2012) [arXiv:1202.0090 [astro-ph.CO]].

[9] C. Blake *et al.*, Mon. Not. Roy. Astron. Soc. **418**, 1707 (2011) [arXiv:1108.2635 [astro-ph.CO]].

[10] L. Anderson *et al.* [BOSS Collaboration], arXiv:1312.4877 [astro-ph.CO].

[11] T. Delubac *et al.* [BOSS Collaboration], arXiv:1404.1801 [astro-ph.CO].

[12] C. Blake *et al.*, Mon. Not. Roy. Astron. Soc. **415**, 2892 (2011) [arXiv:1105.2862 [astro-ph.CO]].

[13] L. Anderson, E. Aubourg, S. Bailey, D. Bizyaev, M. Blanton, A. S. Bolton, J. Brinkmann and J. R. Brownstein *et al.*, Mon. Not. Roy. Astron. Soc. **427**, no. 4, 3435 (2013) [arXiv:1203.6594 [astro-ph.CO]].

[14] N. G. Busca, T. Delubac, J. Rich, S. Bailey, A. Font-Ribera, D. Kirkby, J. M. Le Goff and M. M. Pieri *et al.*, Astron. Astrophys. **552**, A96 (2013) [arXiv:1211.2616 [astro-ph.CO]].

[15] A. Veropalumbo, F. Marulli, L. Moscardini, M. Moresco and A. Cimatti, arXiv:1311.5895 [astro-ph.CO].

[16] M. Manera, R. Scoccimarro, W. J. Percival, L. Samushia, C. K. McBride, A. Ross, R. Sheth and M. White *et al.*, Mon. Not. Roy. Astron. Soc. **428**, no. 2, 1036 (2012) [arXiv:1203.6609 [astro-ph.CO]].

[17] Z. Li, K. Liao, P. Wu, H. Yu and Z. -H. Zhu, Phys. Rev. D **88**, no. 2, 023003 (2013) [arXiv:1306.5932 [gr-qc]].

[18] Y. Zhang and Y. Gong, Mod. Phys. Lett. A **28**, no. 35, 1350135 (2013).

[19] R. Lazkoz, J. Alcaniz, C. Escamilla-Rivera, V. Salzano and I. Sendra, JCAP **1312**, 005 (2013) [arXiv:1311.6817 [astro-ph.CO]].

[20] D. H. Weinberg, M. J. Mortonson, D. J. Eisenstein, C. Hirata, A. G. Riess and E. Rozo, Phys. Rept. **530**, 87 (2013) [arXiv:1201.2434 [astro-ph.CO]].

[21] D. J. Eisenstein and W. Hu, Astrophys. J. **511**, 5 (1997) [astro-ph/9710252].

[22] G. E. Addison, G. Hinshaw and M. Halpern, Mon. Not. Roy. Astron. Soc. **436**, 1674 (2013) [arXiv:1304.6984 [astro-ph.CO]].

[23] E. Aubourg, S. Bailey, J. E. Bautista, F. Beutler, V. Bhardwaj, D. Bizyaev, M. Blanton and M. Blomqvist *et al.*, arXiv:1411.1074 [astro-ph.CO].

[24] C. Cheng and Q. G. Huang, arXiv:1409.6119 [astro-ph.CO].

[25] P. A. R. Ade *et al.* [BICEP2 Collaboration], Phys. Rev. Lett. **112** (2014) 241101 [arXiv:1403.3985 [astro-ph.CO]].

[26] R. Adam *et al.* [Planck Collaboration], arXiv:1409.5738 [astro-ph.CO].

[27] Y. Wang, C. -H. Chuang and P. Mukherjee, Phys. Rev. D **85**, 023517 (2012) [arXiv:1109.3172 [astro-ph.CO]].

[28] Y. Wang and S. Wang, Phys. Rev. D **88**, no. 4, 043522 (2013) [arXiv:1304.4514 [astro-ph.CO]].

[29] A. Lewis and S. Bridle, Phys. Rev. D **66**, 103511 (2002) [astro-ph/0205436].

[30] R. G. Cai, Z. K. Guo and B. Tang, arXiv:1409.0223 [astro-ph.CO].

[31] Z. Li, P. Wu and H. Yu, Astrophys. J. **744**, 176 (2012) [arXiv:1109.6125 [astro-ph.CO]].

[32] A. G. Riess, L. Macri, S. Casertano, H. Lampeitl, H. C. Ferguson, A. V. Filippenko, S. W. Jha and W. Li *et al.*, Astrophys. J. **730**, 119 (2011) [Erratum-ibid. **732**, 129 (2011)] [arXiv:1103.2976 [astro-ph.CO]].

[33] W. L. Freedman, B. F. Madore, V. Scowcroft, C. Burns, A. Monson, S. E. Persson, M. Seibert and J. Rigby, Astrophys. J. **758**, 24 (2012) [arXiv:1208.3281 [astro-ph.CO]].

[34] M. Pettini and R. Cooke, Mon. Not. Roy. Astron. Soc. **425**, 2477 (2012) [arXiv:1205.3785 [astro-ph.CO]].

The ΛCDM Model				
	Ω_m	-	H_0	$r_s H_0$
Planck/BAO	$0.256^{+0.030+0.039}_{-0.010-0.016}$	-	-	-
WMAP9/BAO	$0.277^{+0.031+0.041}_{-0.015-0.021}$	-	-	-
WMAP9(w)/BAO	$0.277^{+0.031+0.040}_{-0.015-0.021}$	-	-	-
Planck/BAO+$\Omega_m h^2$	$0.271^{+0.017+0.027}_{-0.011-0.018}$	-	$66.6^{+1.8+2.9}_{-2.5-3.7}$	-
WMAP9/BAO+$\Omega_m h^2$	$0.293^{+0.018+0.029}_{-0.013-0.020}$	-	$64.0^{+1.8+2.9}_{-2.3-3.3}$	-
WMAP9(w)/BAO+$\Omega_m h^2$	$0.292^{+0.020+0.025}_{-0.013-0.020}$	-	$64.1^{+1.8+2.9}_{-2.2-3.4}$	-
BAO	$0.258^{+0.039+0.066}_{-0.035-0.054}$	-	$42.8^{+47.2+47.2}_{-4.2-4.5}$	$0.978^{+0.216+0.233}_{-0.137-0.150}$
BAO+$\Omega_b h^2$	$0.258^{+0.049+0.076}_{-0.042-0.061}$	-	$66.2^{+3.7+5.8}_{-3.2-4.6}$	$1.031^{+0.046+0.071}_{-0.043-0.063}$
BAO+Planck/BAO	$0.273^{+0.016+0.025}_{-0.013-0.020}$	-	$44.9^{+45.1+45.1}_{-5.7-5.7}$	$1.019^{+0.178+0.193}_{-0.158-0.158}$
BAO+Planck/BAO+$\Omega_b h^2$	$0.275^{+0.016+0.024}_{-0.015-0.022}$	-	$67.5^{+2.5+3.9}_{-2.5-3.6}$	$1.044^{+0.043+0.066}_{-0.043-0.064}$
BAO+Planck/BAO+$\Omega_b h^2$+$\Omega_m h^2$	$0.271^{+0.011+0.016}_{-0.010-0.015}$	-	$66.7^{+1.4+2.1}_{-1.4-2.1}$	$1.033^{+0.034+0.051}_{-0.034-0.050}$
BAO+WMAP9/BAO	$0.287^{+0.017+0.025}_{-0.013-0.020}$	-	$45.9^{+44.1+44.1}_{-6.5-6.5}$	$1.027^{+0.164+0.180}_{-0.159-0.159}$
BAO+WMAP9/BAO+$\Omega_b h^2$	$0.290^{+0.016+0.024}_{-0.015-0.022}$	-	$68.1^{+2.6+4.0}_{-2.5-3.7}$	$1.042^{+0.045+0.067}_{-0.044-0.063}$
BAO+WMAP9/BAO+$\Omega_b h^2$+$\Omega_m h^2$	$0.280^{+0.011+0.016}_{-0.010-0.015}$	-	$66.0^{+1.4+2.1}_{-1.4-2.0}$	$1.014^{+0.034+0.050}_{-0.033-0.049}$
The wCDM Model				
	Ω_m	w	H_0	$r_s H_0$
Planck/BAO	$0.261^{+0.026+0.035}_{-0.029-0.043}$	$-1.095^{+0.295+0.419}_{-0.342-0.541}$	-	-
WMAP9/BAO	$0.266^{+0.036+0.051}_{-0.028-0.044}$	$-1.164^{+0.292+0.426}_{-0.417-0.659}$	-	-
WMAP9(w)/BAO	$0.267^{+0.037+0.051}_{-0.027-0.044}$	$-1.139^{+0.284+0.420}_{-0.435-0.667}$	-	-
Planck/BAO+$\Omega_m h^2$	$0.263^{+0.026+0.036}_{-0.030-0.046}$	$-1.110^{+0.308+0.434}_{-0.414-0.602}$	$67.5^{+4.4+7.1}_{-3.6-4.6}$	-
WMAP9/BAO+$\Omega_m h^2$	$0.277^{+0.033+0.047}_{-0.036-0.054}$	$-1.232^{+0.354+0.496}_{-0.440-0.681}$	$65.9^{+4.9+7.9}_{-3.9-5.3}$	-
WMAP9(w)/BAO+$\Omega_m h^2$	$0.277^{+0.032+0.044}_{-0.036-0.054}$	$-1.217^{+0.350+0.492}_{-0.437-0.682}$	$65.8^{+4.9+7.8}_{-3.7-5.2}$	-
BAO	$0.262^{+0.049+0.073}_{-0.058-0.143}$	$-1.112^{+0.442+0.654}_{-0.530-0.810}$	$70.6^{+19.4+19.4}_{-34.5-34.5}$	$1.098^{+0.322+0.443}_{-0.364-0.413}$
BAO+$\Omega_b h^2$	$0.263^{+0.055+0.081}_{-0.074-0.192}$	$-1.122^{+0.516+0.703}_{-0.609-0.877}$	$69.2^{+13.9+20.5}_{-15.1-23.3}$	$1.096^{+0.335+0.507}_{-0.297-0.460}$
BAO+Planck/BAO	$0.265^{+0.023+0.033}_{-0.022-0.032}$	$-1.121^{+0.224+0.317}_{-0.275-0.408}$	$50.9^{+39.1+39.1}_{-10.4-11.7}$	$1.096^{+0.246+0.310}_{-0.183-0.250}$
BAO+Planck/BAO+$\Omega_b h^2$	$0.267^{+0.025+0.034}_{-0.025-0.036}$	$-1.132^{+0.255+0.349}_{-0.304-0.441}$	$70.1^{+6.7+9.7}_{-5.9-8.1}$	$1.111^{+0.176+0.259}_{-0.141-0.190}$
BAO+Planck/BAO+$\Omega_b h^2$+$\Omega_m h^2$	$0.267^{+0.022+0.031}_{-0.024-0.035}$	$-1.042^{+0.196+0.267}_{-0.242-0.357}$	$67.3^{+3.6+5.4}_{-3.0-4.2}$	$1.051^{+0.116+0.173}_{-0.090-0.120}$
BAO+WMAP9/BAO	$0.275^{+0.024+0.035}_{-0.025-0.036}$	$-1.219^{+0.254+0.360}_{-0.312-0.473}$	$47.2^{+42.8+42.8}_{-7.4-7.4}$	$1.123^{+0.262+0.333}_{-0.236-0.236}$
BAO+WMAP9/BAO+$\Omega_b h^2$	$0.276^{+0.026+0.037}_{-0.028-0.040}$	$-1.240^{+0.296+0.406}_{-0.341-0.498}$	$72.7^{+7.1+10.5}_{-6.5-8.9}$	$1.163^{+0.190+0.289}_{-0.156-0.214}$
BAO+WMAP9/BAO+$\Omega_b h^2$+$\Omega_m h^2$	$0.278^{+0.022+0.031}_{-0.024-0.035}$	$-1.009^{+0.197+0.268}_{-0.256-0.375}$	$66.1^{+3.6+5.3}_{-2.8-3.9}$	$1.018^{+0.113+0.168}_{-0.083-0.113}$
The oΛCDM Model				
	Ω_m	Ω_k	H_0	$r_s H_0$
Planck/BAO	$0.259^{+0.038+0.066}_{-0.037-0.057}$	$-0.010^{+0.034+0.051}_{-0.020-0.028}$	-	-
WMAP9/BAO	$0.259^{+0.041+0.070}_{-0.036-0.056}$	$-0.025^{+0.036+0.054}_{-0.016-0.024}$	-	-
WMAP9(w)/BAO	$0.262^{+0.041+0.069}_{-0.038-0.057}$	$-0.022^{+0.035+0.052}_{-0.015-0.025}$	-	-
Planck/BAO+$\Omega_m h^2$	$0.257^{+0.049+0.077}_{-0.041-0.059}$	$-0.009^{+0.031+0.049}_{-0.024-0.032}$	$68.3^{+6.4+9.9}_{-5.9-8.6}$	-
WMAP9/BAO+$\Omega_m h^2$	$0.259^{+0.050+0.079}_{-0.043-0.061}$	$-0.021^{+0.030+0.047}_{-0.022-0.029}$	$68.0^{+6.6+10.2}_{-5.9-8.6}$	-
WMAP9(w)/BAO+$\Omega_m h^2$	$0.262^{+0.051+0.079}_{-0.044-0.062}$	$-0.018^{+0.029+0.047}_{-0.023-0.031}$	$67.7^{+6.6+10.1}_{-5.9-8.6}$	-
BAO	$0.268^{+0.051+0.077}_{-0.058-0.094}$	$-0.103^{+0.391+0.653}_{-0.256-0.343}$	$76.0^{+14.0+14.0}_{-38.9-38.9}$	$1.131^{+0.247+0.320}_{-0.358-0.365}$
BAO+$\Omega_b h^2$	$0.266^{+0.059+0.085}_{-0.064-0.096}$	$-0.097^{+0.438+0.688}_{-0.285-0.368}$	$69.2^{+12.9+18.1}_{-12.4-17.4}$	$1.096^{+0.259+0.360}_{-0.252-0.349}$
BAO+Planck/BAO	$0.259^{+0.033+0.051}_{-0.030-0.043}$	$-0.021^{+0.021+0.031}_{-0.016-0.023}$	$86.3^{+3.7+3.7}_{-45.2-46.9}$	$1.154^{+0.056+0.072}_{-0.222-0.281}$
BAO+Planck/BAO+$\Omega_b h^2$	$0.258^{+0.040+0.058}_{-0.033-0.045}$	$-0.021^{+0.023+0.034}_{-0.018-0.024}$	$66.6^{+3.7+5.3}_{-3.2-4.5}$	$1.042^{+0.052+0.074}_{-0.047-0.067}$
BAO+Planck/BAO+$\Omega_b h^2$	$0.265^{+0.017+0.024}_{-0.016-0.022}$	$-0.017^{+0.014+0.020}_{-0.013-0.018}$	$67.2^{+1.9+2.7}_{-1.9-2.6}$	$1.047^{+0.046+0.066}_{-0.046-0.065}$
BAO+WMAP9/BAO	$0.260^{+0.033+0.051}_{-0.030-0.043}$	$-0.021^{+0.021+0.032}_{-0.016-0.022}$	$86.0^{+4.0+4.0}_{-44.9-46.4}$	$1.151^{+0.059+0.073}_{-0.214-0.277}$
BAO+WMAP9/BAO+$\Omega_b h^2$	$0.259^{+0.039+0.057}_{-0.034-0.046}$	$-0.020^{+0.023+0.033}_{-0.018-0.024}$	$66.7^{+3.6+5.3}_{-3.3-4.6}$	$1.044^{+0.050+0.073}_{-0.049-0.069}$
BAO+WMAP9/BAO+$\Omega_b h^2$+$\Omega_m h^2$	$0.265^{+0.017+0.024}_{-0.015-0.022}$	$-0.018^{+0.014+0.020}_{-0.012-0.018}$	$67.3^{+1.8+2.6}_{-1.9-2.7}$	$1.048^{+0.046+0.065}_{-0.047-0.066}$

Table 2: The constraining results for the ΛCDM, oΛCDM and wCDM models.